Inorganic Chemistry

ARTICLE

pubs.acs.org/IC

Systematic Modulation of a Bichromic Cyclometalated Ruthenium(II) Scaffold Bearing a Redox-Active Triphenylamine Constituent

Kiyoshi C. D. Robson,[†] Barbora Sporinova,[†] Bryan D. Koivisto,[†] Eduardo Schott,[‡] Douglas G. Brown,[†] and Curtis P. Berlinguette*[,†]

[†]Department of Chemistry and Institute for Sustainable Energy, Environment and Economy, University of Calgary, 2500 University Drive NW, Calgary, Canada T2N 1N4

[‡]Departamento de Ciencias Químicas, Universidad Andres Bello, República 275, Santiago, Chile

Supporting Information

ABSTRACT: The syntheses and physicochemical properties of nine bis-tridentate ruthenium(II) complexes containing one cyclometalating ligand furnished with terminal triphenylamine (TPA) substituents are reported. The structure of each complex conforms to a molecular scaffold formulated as [Ru^{II}(TPA-2,5-thiophene-pbpy)(Me_3tctpy)] (pbpy = 6-phenyl-2,2′-bipyridine; Me_3tctpy = trimethyl-4,4′,4″-tricarboxylate-2,2′:6′,2″-terpyridine), where various electron-donating groups (EDGs) and electron-withdrawing groups (EWGs) are installed about the TPA unit and the anionic ring of the pbpy ligand. It is found that the redox chemistry of the Ru center and the TPA unit can be independently modulated by (i) placing EWGs (e.g., $-CF_3$) or EDGs (e.g., $-OMe$) on the anionic ring of the pbpy ligand (substituted sites denoted as R_2 or R_3) and/or (ii) installing electron-donating substituents (e.g., $-H$, $-Me$, $-OMe$) para to the amine of the TPA group (i.e., R_1). The first oxidation potential is localized to the TPA unit when, for example, EDGs are placed at R_1 with EWGs at R_2 (e.g., the $TPA^{\bullet+}/TPA^0$ and Ru^{III}/Ru^{II} redox couples appear at +0.98 and +1.27 V vs NHE, respectively, when $R_1 = -OMe$ and $R_2 = -CF_3$). This situation is reversed when R_3 = EDG and $R_1 = -H$: TPA-based and metal-centered oxidation waves occur at +1.20 and +1.11 V vs NHE, respectively. The UV−vis spectrum for each complex is broad (e.g., absorption bands are extended from the UV region to beyond 800 nm in all cases) and intense (e.g., $\varepsilon \sim 10^4$ $M^{-1}\cdot cm^{-1}$) because of the overlapping intraligand charge-transfer and metal-to-ligand charge-transfer transitions. The information derived from this study offers guiding principles for modulating the physicochemical properties of bichromic cyclometalated ruthenium(II) complexes.

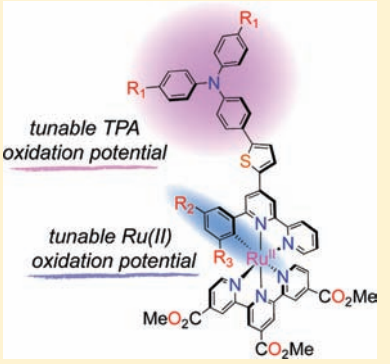

INTRODUCTION

Cyclometalated ruthenium(II) complexes have recently emerged as a promising class of sensitizers for use in dye-sensitized solar cells (DSSCs).[1−7] Indeed, complexes formulated as [Ru(dcbpy)$_2$($C^\wedge N$)]$^+$ [dcbpy = 4,4′-dicarboxy-2,2″-bipyridine; $C^\wedge N$ = cyclometalating ligand (e.g., 2-phenylpyridine)] have proven to be viable alternatives to conventional high-performance ruthenium-based dyes [e.g., [Ru(dcbpy)$_2$($NCS)_2$] (**N3**)][8] because of their broad absorbance profiles and suitable ground- and excited-state oxidation potentials.[4,5] Moreover, cyclometalated derivatives offer a significant advantage over conventional dyes in that the absence of NCS^- ligands about the Ru center circumvents access to significant degradation pathways within an operating cell; e.g., the monodentate NCS^- groups can be displaced by additives in the electrolyte.[9] The first documented DSSC containing a cyclometalated Ru sensitizer was provided by van Koten et al. in the form of a bis-tridentate complex [e.g., [Ru^{II}(tpy)-(pdcbpy)]$^+$ (tpy = 2,2′:6′,2″-terpyridine; pdcbpy = 4,4′-dicarboxy-6-phenyl-2,2′-bipyridine].[3] While the performance of this dye in the DSSC was modest, we have shown that derivatives of this complex can exceed power conversion efficiencies (η) of 8%.[10] Moreover, independent report by Grätzel et al., demonstrated that the cyclometalated complex [Ru(dcbpyH$_2$)$_2$(ppyF$_2$)]$^+$ [ppyF$_2$ = 2-(2,4-difluorophenyl)pyridine] could generate power conversion efficiencies in excess of 10.1%.[4] This result has heralded a new paradigm of dye development because it represents the first "champion" (i.e., η > 10%) dye devoid of NCS^- groups.[2,11−16]

Building on these and related studies by Sauvage et al.,[17−20] Hammarström et al.,[13,21,22] and others,[23−26] our program has focused exclusively on systematically modulating bidentate and tridentate cyclometalated ruthenium(II) complexes to gain a fundamental understanding of how to modulate the optical and electrochemical properties of this class of dyes. In general, cyclometalated ruthenium complexes contain a highest occupied molecular orbital (HOMO) that is extended over the metal and anionic portion of the cyclometalating ligand.[5,15,27−31] Because the lowest unoccupied molecular orbital (LUMO) is localized to the neutral polypyridyl ligands, a series of broad absorption bands in the visible region arise from a suite of mixed-metal-ligand-to-ligand charge-transfer transitions.[15,32] Notably, these

Received: December 24, 2010
Published: June 09, 2011

Chart 1. Designation of Compounds[a]

Complex	Ligand	Substituent		
		-R_1	-R_2	-R_3
1	L1	-H	-H	-H
2	L2	-Me	-H	-H
3	L3	-OMe	-H	-H
4	L4	-H	-CF_3	-H
5	L5	-Me	-CF_3	-H
6	L6	-OMe	-CF_3	-H
7	L7	-H	-H	-OMe
8	L8	-Me	-H	-OMe
9	L9	-OMe	-H	-OMe

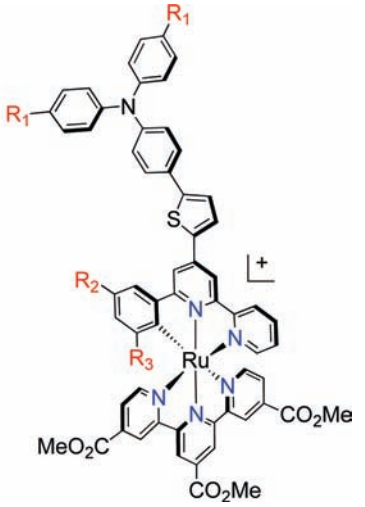

[a]Counterion = NO_3^- for **1**−**9**.

transitions also position the excited-state electron density on the polypyridyl ligand attached to the semiconductor to enable rapid and efficient charge injection into a TiO_2 collecting electrode.[5,33−35] Moreover, replacement of the NCS^- groups with a cyclometalating ligand offers the unique opportunity to independently tune *both* the metal-based HOMO and the ligand π^*-based LUMO.[28,36]

To further expand on this chemistry, we have set out to consolidate these organometallic dyes[8,37−42] with organic triphenylamine (TPA) fragments[43−46] as a means of generating broad, intense absorbance bands in the visible region. While bistridentate polypyridylruthenium complexes containing TPA donor units are known,[47,48] they are not ideal for sensitizing TiO_2 because of a relatively narrow absorption band coupled with a low π^* energy level.[33,49] An examination of heteroleptic cyclometalated ruthenium(II) bichromic complexes disclosed in our previous study demonstrated that cyclometalating ligands serve to desymmetrize the local geometry and raise the filled frontier orbitals to induce a broad spectral profile extending beyond 800 nm, while pushing up the π^* energy levels to enhance the possibility for electron injection into TiO_2.[10] Moreover, we have found that the TPA and metal-based chromophores exist as electrochemically independent units, thereby offering acute control of each of the chromophore units.

Our previous work identified that the optimal dye motif for sensitizing TiO_2 is the situation where the organometallic bond is located cis to the central ring of the tridentate TPA-bearing ligand (e.g., Chart 1).[10] Not only does this arrangement balance light absorption and electron-injection events, it also provides the opportunity to induce an electronic cascade effect that effectively shuttles holes away from the surface.[47,50−54] Under the auspices of these motivating factors, we detail herein our efforts to further develop the molecular platform in Chart 1 to examine how the optical and electrochemical properties are affected by terminal substituents at *both* TPA (e.g., R_1) and the metal chelate (e.g., R_2 and R_3). This family of bichromic dyes reveals that the ruthenium-based redox potential can be tuned independently of the TPA redox potential by substitution of the R_2/R_3 positions of the pbpy chelate with electron-withdrawing groups (EWGs; i.e., $-CF_3$) or electron-donating groups (EDGs; i.e., −OMe). Similarly, tuning of the $TPA^{\bullet+}/TPA^0$ oxidation potential can be achieved by substitution (e.g., −H, −Me, −OMe) at the R_1 site of the TPA without affecting the metal-based redox potentials. Systematic substitution of these two chromophore units reveals that the electrochemical behavior can be adjusted such that the HOMO resides on either the metal or the TPA unit. This control over the relative energy alignment between the two chromophores offers another handle for optimizing this class of dyes for the DSSC and presents a promising route for developing "black dye" analogues that are devoid of NCS^- groups.[55]

EXPERIMENTAL SECTION

Preparation of Compounds. All reactions and manipulations were performed using solvents passed through an MBraun solvent purification system prior to use. All reagents were purchased from Aldrich except for $RuCl_3 \cdot 3H_2O$ (Pressure Chemical Co., Pittsburgh, PA) and trimethyl-4,4′,4″-tricarboxylate-2,2′:6′,2″-terpyridine (**L10**; Helios Chemical Co., Ecublens, Switzerland). Purification by column chromatography was carried out using silica (silicycle: ultrapure flash silica). Analytical thin-layer chromatography was performed on aluminum-backed sheets precoated with silica 60 F254 adsorbent (0.25 mm thick; Merck, Darmstadt, Germany) and visualized under UV light. Routine ^1H and ^{13}C NMR spectra were recorded at 400 and 100 MHz, respectively, on a Bruker AV 400 instrument at ambient temperature. Chemical shifts (δ) are reported in parts per million (ppm) from low to high field and referenced to a residual nondeuterated solvent. Standard abbreviations indicating multiplicity are used as follows: s = singlet; d = doublet; t = triplet; m = multiplet. All proton assignments correspond to the generic molecular schemes that are provided (Figure 1). Organic compounds *N*,*N*-diphenyl-4-(4,4,5,5-tetramethyl-1,3,2-dioxaborolan-2-yl)aniline (**P1**),[56] 4-methyl-*N*-[4-(4,4,5,5-tetramethyl-1,3,2-dioxaborolan-2-yl)phenyl]-*N*-*p*-tolylaniline (**P2**),[57] 4-methoxy-*N*-(4-methoxyphenyl)-*N*-[4-(4,4,5,5-tetramethyl-1,3,2-dioxaborolan-2-yl)phenyl]aniline (**P3**),[58] 4-(5-bromothiophen-2-yl)-6-phenyl-2,2′-bipyridine (**P4**),[10] *N*,*N*-diphenyl-4-[5-(6-phenyl-2,2′-bipyridin-4-yl)thiophen-2-yl]aniline (**L1H**),[10] 4-methyl-*N*-[4-[5-(6-phenyl-2,2′-bipyridin-4-yl)thiophen-2-yl]phenyl]-*N*-*p*-tolylaniline (**L2H**),[10] 4-methoxy-*N*-(4-methoxyphenyl)-*N*-[4-[5-(6-phenyl-2,2′-bipyridin-4-yl)thiophen-2-yl]phenyl]aniline (**L3H**),[10] and 6-phenyl-2,2′-bipyridine (pbpy)[5] were prepared as previously reported. Complexes **1**−**3** were also prepared as previously reported.[10]

dx.doi.org/10.1021/ic1025679 |*Inorg. Chem.* 2011, 50, 6019–6028

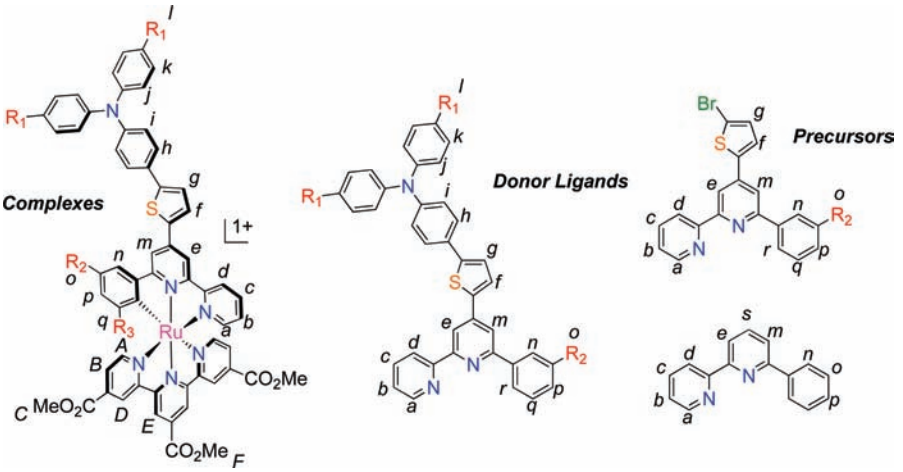

Figure 1. Generic labeling scheme for ^{1}H NMR signal assignments.

*4-(5-Bromothiophen-2-yl)-6-[3-(trifluoromethyl)phenyl]-2,2′-bipyridine (**P5**).* A mixture of 1-[2-oxo-2-[3-(trifluoromethyl)phenyl]ethyl]pyridinium iodide[59] (1.34 g, 3.40 mmol), (*E*)-3-(5-bromothiophen-2-yl)-1-(pyridin-2-yl)prop-2-en-1-one[60] (1.00 g, 3.40 mmol), and ammonium acetate (6.81 g, 88.4 mmol) were refluxed in formamide (25 mL) for 14 h. The resulting heterogeneous solution was cooled to room temperature. The solid was removed by filtration, dried, and triturated with methanol (MeOH). The product was dried in vacuo to give 1.15 g (2.49 mmol, 73.3%) of an off-white solid. ^{1}H NMR (400 MHz, $CDCl_3$): δ 8.69 (ddd, 1H, ^3J = 4.8 Hz, ^4J = 1.8 Hz, ^5J = 1.0 Hz, H_a), 8.58 (ddd, 1H, ^3J = 8.0 Hz, ^4J = 1.0 Hz, ^5J = 1.0 Hz, H_d), 8.55 (d, 1H, ^4J = 1.6 Hz, H_e), 8.39 (s, 1H, H_n), 8.28 (d, 1H, ^3J = 7.8 Hz, H_r), 7.86 (dt, 1H, ^3J = 7.9, ^4J = 1.8 Hz, H_c), 7.78 (d, 1H, ^4J = 1.6 Hz, H_m), 7.69 (d, 1H, ^3J = 7.8 Hz, H_p), 7.61 (t, 1H, ^3J = 7.8 Hz, H_q), 7.44 (d, 1H, ^3J = 3.9 Hz, H_f), 7.35 (ddd, 1H, ^3J = 7.5 Hz, ^3J = 4.8 Hz, ^4J = 1.0 Hz, H_b), 7.11 (d, 1H, ^3J = 3.9 Hz, H_g). ^{13}C NMR (100 MHz, $CDCl_3$): δ 156.9, 156.1, 155.7, 149.2, 143.0, 142.9, 140.0, 137.3, 131.5, 131.4 (q, $^2J_{CF}$ = 32.2 Hz), 130.4, 129.5, 126.3, 126.1 (q, $^3J_{CF}$ = 3.9 Hz), 124.5 (q, $^1J_{CF}$ = 272.5 Hz), 124.4, 124.1 (q, $^3J_{CF}$ = 3.9 Hz), 121.7, 116.4, 116.1, 114.7. HRMS (EI): m/z 461.9836 [$(M)^+$] (calcd for $C_{21}H_{12}N_2F_3S^{81}Br^+$: m/z 461.9836).

*4-(5-Bromothiophen-2-yl)-6-(3-methoxyphenyl)-2,2′-bipyridine (**P6**).* A mixture of 1-[2-(3-methoxyphenyl)-2-oxoethyl]pyridinium iodide[61] (1.81 g, 5.10 mmol), (*E*)-3-(5-bromothiophen-2-yl)-1-(pyridin-2-yl)-prop-2-en-1-one[60] (1.50 g, 5.10 mmol), and ammonium acetate (10.22 g, 133 mmol) were refluxed in formamide (25 mL) for 14 h. After the resultant heterogeneous solution was cooled to room temperature, the solid was removed by filtration, dried, and triturated with MeOH. The product was dried in vacuo to give 1.49 g (3.52 mmol, 69.0%) of an off-white solid. ^{1}H NMR (400 MHz, $CDCl_3$): δ 8.69 (ddd, 1H, ^3J = 4.8 Hz, ^4J = 1.8 Hz, ^5J = 1.0 Hz, H_a), 8.61 (ddd, 1H, ^3J = 8.0 Hz, ^4J = 1.0 Hz, ^5J = 1.0 Hz, H_d), 8.51 (d, 1H, ^4J = 1.6 Hz, H_e), 7.83 (dt, 1H, ^3J = 7.8 Hz, ^4J = 1.8 Hz, H_c), 7.78 (d, 1H, ^4J = 1.6 Hz, H_m), 7.73 (t, 1H, ^4J = 1.6 Hz, H_n), 7.68 (dd, 1H, ^3J = 7.9 Hz, ^4J = 1.6 Hz, H_r), 7.43 (d, 1H, ^3J = 3.9 Hz, H_f), 7.42 (t, 1H, ^3J = 7.9 Hz, H_q), 7.32 (ddd, 1H, ^3J = 7.5 Hz, ^3J = 4.8 Hz, ^4J = 1.0 Hz, H_b), 7.10 (d, 1H, ^3J = 3.9 Hz, H_g), 6.99 (ddd, 1H, ^3J = 7.9 Hz, ^4J = 1.8 Hz, ^4J = 1.0 Hz, H_p), 3.91 (s, 3H, H_o). ^{13}C NMR (100 MHz, $CDCl_3$): δ 160.3, 157.3, 156.7, 156.0, 149.2, 143.4, 142.5, 140.7, 137.1, 131.4, 129.9, 125.9, 124.2, 121.6, 119.6, 116.5, 115.5, 114.9, 114.3, 113.0, 55.6. HRMS (EI): m/z 422.9981 [$(M)^+$] (calcd for $C_{21}H_{14}N_2OS^{81}Br^+$: m/z 422.9990).

General Preparation of Ligands L1H−L9H. Boronic esters (**P1**−**P3**; 1.67 mmol) and bromides (**P4**−**P6**; 1.50 mmol) were solubilized in a tetrahydrofuran (THF)/water solution (9:1; 130 mL) and sparged for 10 min with nitrogen. K_2CO_3 (8.75 mmol) and $Pd(PPh_3)_4$ (0.15 mmol) were then added to the reaction solution, which was then refluxed for 14 h under nitrogen. The reaction mixture was then cooled, and the THF layer was washed with brine. The organic fractions were isolated after being dried with $MgSO_4$. The resultant oil was purified by column chromatography and then triturated with MeOH to yield the target ligand as a solid; specific details are given below.

*N,N-Diphenyl-4-[5-[6-[3-(trifluoromethyl)phenyl]-2,2′-bipyridin-4-yl]thiophen-2-yl]aniline (**L4H**).* Proligands: **P1** and **P5**. Column chromatography: SiO_2; CH_2Cl_2, R_f = 0.60. Yield: 853 mg (1.36 mmol, 81.6%); yellow-green solid. ^{1}H NMR (400 MHz, $CDCl_3$): δ 8.70 (ddd, 1H, ^3J = 4.7 Hz, ^4J = 1.6 Hz, ^5J = 0.8 Hz, H_a), 8.59 (d, 1H, ^4J = 1.6 Hz, H_e), 8.57 (d, 1H, ^3J = 7.9 Hz, H_d), 8.43 (s, 1H, H_n), 8.28 (d, 1H, ^3J = 7.9 Hz, H_r), 7.83 (d, 1H, ^4J = 1.6 Hz, H_m), 7.81 (dt, 1H, ^3J = 7.7 Hz, ^4J = 1.6 Hz, H_c), 7.68 (d, 1H, ^3J = 7.9 Hz, H_p), 7.58 (t, 1H, ^3J = 7.9 Hz, H_q), 7.57 (d, 1H, ^3J = 3.9 Hz, H_f), 7.48 (d, 2H, ^3J = 8.8 Hz, H_h), 7.33−7.25 (m, 5H, H_b, H_k), 7.21 (d, 1H, ^3J = 3.9 Hz, H_g), 7.14 (d, 4H, ^3J = 9.0 Hz, H_j), 7.09−7.04 (m, 4H, H_i, H_l), ^{13}C NMR (100 MHz, $CDCl_3$): δ 156.8, 156.0, 155.8, 149.3, 148.1, 147.5, 146.5, 143.6, 140.3, 139.5, 137.1, 131.4 (q, $^2J_{CF}$ = 32.3 Hz), 130.4, 129.6, 129.5, 129.4, 127.7, 127.1, 126.8, 125.9 (q, $^3J_{CF}$ = 3.8 Hz), 125.0, 124.4 (q, $^1J_{CF}$ = 272.3 Hz), 124.2, 124.1 (q, $^3J_{CF}$ = 3.9 Hz), 123.6, 123.5, 121.6, 116.3, 116.0. HRMS (ESI): m/z 626.1875 [$(MH)^+$] (calcd for $C_{39}H_{27}F_3N_3S^+$: m/z 626.1872).

*4-Methyl-N-p-tolyl-N-[4-[5-[6-[3-(trifluoromethyl)phenyl]-2,2′-bipyridin-4-yl]thiophene-2-yl]phenyl]aniline (**L5H**).* Proligands: **P2** and **P5**. Column chromatography: SiO_2; CH_2Cl_2, R_f = 0.54. Yield: 734 mg (1.12 mmol, 67.4%); yellow solid. ^{1}H NMR (400 MHz, $CDCl_3$): δ 8.71 (ddd, 1H, ^3J = 4.7 Hz, ^4J = 1.6 Hz, ^5J = 0.8 Hz, H_a), 8.64 (d, 1H, ^4J = 1.6 Hz, H_e), 8.61 (dt, 1H, ^3J = 7.9 Hz, ^4J = 1.0 Hz, H_d), 8.44 (s, 1H, H_n), 8.33 (d, 1H, ^3J = 7.9 Hz, H_r), 7.91 (d, 1H, ^4J = 1.6 Hz, H_m), 7.85 (dt, 1H, ^3J = 7.7 Hz, ^4J = 1.6 Hz, H_c), 7.70 (d, 1H, ^3J = 7.9 Hz, H_p), 7.65 (d, 1H, ^3J = 3.9 Hz, H_f), 7.62 (t, 1H, ^3J = 7.9 Hz, H_q), 7.48 (d, 2H, ^3J = 8.8 Hz, H_h), 7.35 (ddd, 1H, ^3J = 7.5 Hz, ^3J = 4.8 Hz, ^4J = 1.0 Hz, H_b), 7.25 (d, 1H, ^3J = 3.9 Hz, H_g), 7.08 (d, 4H, ^3J = 8.2 Hz, H_k), 7.04−6.99 (m, 6H, H_i, H_j), 2.32 (s, 6H, H_l). ^{13}C NMR (100 MHz, $CDCl_3$): δ 156.7, 156.0, 155.8, 149.2, 148.5, 146.7, 145.0, 143.7, 140.3, 139.2, 137.2, 133.3, 131.3 (q, $^2J_{CF}$ = 32.3 Hz), 130.4, 130.2, 129.4, 127.1, 126.8, 126.7, 125.8 (q, $^3J_{CF}$ = 3.8 Hz), 125.2, 124.5 (q, $^1J_{CF}$ = 272.3 Hz), 124.2, 124.1 (q, $^3J_{CF}$ = 3.9 Hz), 123.2, 122.2, 121.7, 116.2, 116.0, 21.1. HRMS (ESI): m/z 654.2184 [$(MH)^+$] (calcd for $C_{41}H_{31}F_3N_3S^+$: m/z 654.2185).

*4-Methoxy-N-(4-methoxyphenyl)-N-[4-[5-[6-[3-(trifluoromethyl)-phenyl]-2,2′-bipyridin-4-yl]thiophen-2-yl]phenyl]aniline (**L6H**).* Proligands: **P3** and **P5**. Column chromatography: SiO_2; CH_2Cl_2, R_f = 0.33. Yield: 845 mg (1.23 mmol, 73.8%); yellow-orange solid. ^{1}H NMR (400 MHz, $CDCl_3$): δ 8.72 (ddd, 1H, ^3J = 4.7 Hz, ^4J = 1.6 Hz, ^5J = 0.8 Hz, H_a),

8.63 (d, 1H, ^4J = 1.6 Hz, H_e), 8.61 (dt, 1H, ^3J = 7.9 Hz, ^4J = 1.0 Hz, H_d), 8.43 (s, 1H, H_n), 8.32 (d, 1H, ^3J = 7.9 Hz, H_r), 7.89 (d, 1H, ^4J = 1.6 Hz, H_m), 7.86 (dt, 1H, ^3J = 7.7 Hz, ^4J = 1.6 Hz, H_c), 7.69 (d, 1H, ^3J = 7.9 Hz, H_p), 7.64 (d, 1H, ^3J = 3.9 Hz, H_f), 7.62 (t, 1H, ^3J = 7.9 Hz, H_q), 7.45 (d, 2H, ^3J = 8.8 Hz, H_h), 7.34 (ddd, 1H, ^3J = 7.5 Hz, ^3J = 4.8 Hz, ^4J = 1.0 Hz, H_b), 7.21 (d, 1H, ^3J = 3.9 Hz, H_g), 7.08 (d, 4H, ^3J = 8.2 Hz, H_k), 6.92 (d, 2H, ^3J = 8.8 Hz, H_i), 6.84 (d, 4H, ^3J = 8.2 Hz, H_j), 3.72 (s, 6H, H_l). ^{13}C NMR (100 MHz, $CDCl_3$): δ 156.7, 156.4, 156.0, 155.8, 149.2, 149.1, 147.0, 143.8, 140.6, 140.3, 138.9, 137.2, 131.4 (q, $^2J_{CF}$ = 32.3 Hz), 130.4, 129.4, 127.1, 127.0, 126.7, 125.9 (q, $^3J_{CF}$ = 3.8 Hz), 125.8, 124.5 (q, $^1J_{CF}$ = 272.3 Hz), 124.3, 124.1 (q, $^3J_{CF}$ = 3.9 Hz), 123.0, 121.7, 120.3, 116.3, 116.0, 115.0, 55.7. HRMS (ESI): m/z 686.2085 [$(MH)^+$] (calcd for $C_{41}H_{31}F_3N_3O_2S^+$: m/z 686.2084).

*4-[5-[6-(3-Methoxyphenyl)-2,2′-bipyridin-4-yl]thiophen-2-yl]-N,N-diphenylaniline (**L7H**).* Proligands: **P1** and **P6**. Column chromatography: SiO_2; CH_2Cl_2, R_f = 0.33. Yield: 724 mg (1.23 mmol, 74.2%); yellow-orange solid. ^{1}H NMR (400 MHz, $CDCl_3$): δ 8.72 (ddd, 1H, ^3J = 4.8 Hz, ^4J = 1.8 Hz, ^5J = 1.0 Hz, H_a), 8.64 (ddd, 1H, ^3J = 8.0 Hz, ^4J = 1.0 Hz, ^5J = 1.0 Hz, H_d), 8.61 (d, 1H, ^4J = 1.6 Hz, H_e), 7.90 (d, 1H, ^4J = 1.6 Hz, H_m), 7.83 (dt, 1H, ^3J = 7.7 Hz, ^4J = 1.6 Hz, H_c), 7.78 (dd, 1H, ^4J = 1.5 and 1.0 Hz, H_n), 7.73 (dt, 1H, ^3J = 7.9 Hz, ^4J = 1.6 Hz, H_r), 7.63 (d, 1H, ^3J = 3.9 Hz, H_f), 7.51 (d, 2H, ^3J = 8.9 Hz, H_h), 7.43 (t, 1H, ^3J = 7.9 Hz, H_q), 7.32 (ddd, 1H, ^3J = 7.5 Hz, ^3J = 4.8 Hz, ^4J = 1.0 Hz, H_b), 7.31−7.24 (m, 5H, H_k, H_g), 7.13 (d, 4H, ^3J = 8.1 Hz, H_j), 7.10−7.04 (m, 4H, H_i, H_l), 7.00 (ddd, 1H, ^3J = 7.9 Hz, ^4J = 1.8 Hz, ^4J = 1.0 Hz, H_p), 3.93 (s, 3H, H_o). ^{13}C NMR (100 MHz, $CDCl_3$): δ 160.3, 157.2, 156.5, 156.3, 149.2, 148.0, 147.6, 146.2, 143.4, 141.0, 139.9, 137.1, 135.3, 129.9, 129.6, 128.3, 127.9, 126.8, 124.9, 124.1, 123.6, 123.5, 121.7, 119.7, 116.5, 115.5, 114.8, 113.1, 55.6. HRMS (EI): m/z 587.2059 [$(M)^+$] (calcd for $C_{39}H_{29}N_3OS^+$: m/z 587.2031).

*4-[5-[6-(3-Methoxyphenyl)-2,2′-bipyridin-4-yl]thiophen-2-yl]-N,N-di-p-tolylaniline (**L8H**).* Proligands: **P2** and **P6**. Column chromatography: SiO_2; CH_2Cl_2, R_f = 0.21. Yield: 665 mg (1.08 mmol, 64.8%); yellow-green solid. ^{1}H NMR (400 MHz, $CDCl_3$): δ 8.71 (dd, 1H, ^3J = 4.8 Hz, ^4J = 1.5 Hz, H_a), 8.63 (d, 1H, ^3J = 7.5 Hz, H_d), 8.59 (d, 1H, ^4J = 1.6 Hz, H_e), 7.89 (d, 1H, ^4J = 1.6 Hz, H_m), 7.83 (dt, 1H, ^3J = 7.7 Hz, ^4J = 1.6 Hz, H_c), 7.78 (t, 1H, ^4J = 1.0 Hz, H_n), 7.72 (d, 1H, ^3J = 7.9 Hz, H_r), 7.63 (d, 1H, ^3J = 3.9 Hz, H_f), 7.47 (d, 2H, ^3J = 8.9 Hz, H_h), 7.43 (t, 1H, ^3J = 7.9 Hz, H_q), 7.32 (ddd, 1H, ^3J = 7.5 Hz, ^3J = 4.8 Hz, ^4J = 1.0 Hz, H_b), 7.22 (d, 1H, ^3J = 3.9 Hz, H_g), 7.09 (d, 4H, ^3J = 8.1 Hz, H_k), 7.05−6.98 (m, 7H, H_i, H_j, H_p), 3.92 (s, 3H, H_o), 2.32 (s, 6H, H_l). ^{13}C NMR (100 MHz, $CDCl_3$): δ 160.2, 157.2, 156.4, 156.3, 149.2, 148.4, 146.4, 145.1, 143.4, 141.0, 139.6, 137.0, 133.2, 130.2, 129.9, 126.9, 126.8, 126.7, 125.2, 124.0, 123.2, 122.3, 121.7, 119.7, 116.5, 115.5, 114.7, 113.0, 55.6, 21.0. HRMS (ESI): m/z 616.2411 [$(MH)^+$] (calcd for $C_{41}H_{34}N_3OS^+$: m/z 616.2417).

*4-Methoxy-N-(4-methoxyphenyl)-N-[4-[5-[6-(3-methoxyphenyl)-2,2′-bipyridin-4-yl]thiophen-2-yl]phenyl]aniline (**L9H**).* Proligands: **P3** and **P6**. Column chromatography: SiO_2; CH_2Cl_2, R_f = 0.12. Yield: 735 mg (1.13 mmol, 68.0%); orange solid. ^{1}H NMR (400 MHz, $CDCl_3$): δ 8.71 (dd, 1H, ^3J = 4.8 Hz, ^4J = 1.5 Hz, H_a), 8.63 (d, 1H, ^3J = 7.5 Hz, H_d), 8.59 (d, 1H, ^4J = 1.6 Hz, H_e), 7.89 (d, 1H, ^4J = 1.6 Hz, H_m), 7.83 (dt, 1H, ^3J = 7.7 Hz, ^4J = 1.6 Hz, H_c), 7.77 (dd, 1H, ^4J = 1.5 and 1.0 Hz, H_n), 7.72 (dt, 1H, ^3J = 7.9 Hz, ^4J = 1.6 Hz, H_r), 7.63 (d, 1H, ^3J = 3.9 Hz, H_f), 7.45 (d, 2H, ^3J = 8.9 Hz, H_h), 7.42 (t, 1H, ^3J = 7.9 Hz, H_q), 7.32 (ddd, 1H, ^3J = 7.5 Hz, ^3J = 4.8 Hz, ^4J = 1.0 Hz, H_b), 7.21 (d, 1H, ^3J = 3.9 Hz, H_g), 7.08 (d, 4H, ^3J = 8.1 Hz, H_k), 6.99 (ddd, 1H, ^3J = 7.9 Hz, ^4J = 1.8 Hz, ^4J = 1.0 Hz, H_p), 7.08 (d, 2H, ^3J = 8.8 Hz, H_i), 7.08 (d, 4H, ^3J = 8.1 Hz, H_j), 3.92 (s, 3H, H_o), 3.79 (s, 6H, H_l). ^{13}C NMR (100 MHz, $CDCl_3$): δ 160.3, 157.2, 156.5, 156.4, 149.2, 149.0, 146.6, 143.4, 141.1, 140.7, 139.4, 137.0, 129.9, 127.1, 126.8, 126.7, 125.9, 124.1, 122.9, 121.7, 120.4, 119.7, 116.5, 115.4, 115.2, 115.0, 114.7, 113.0, 55.7, 55.6. HRMS (ESI): m/z 648.2323 [$(M)^+$] (calcd for $C_{41}H_{34}N_3O_3S^+$: m/z 648.2315).

General Preparation of Methyl Ester Complexes (1−10). To a MeOH/H_2O/THF solution (5:1:1, v/v/v, 280 mL) containing 0.40 mmol of the ligand (e.g., **L1H**−**L9H** and **L12H**) were added 0.4 mmol of Ru(**L10**)Cl_3 and *N*-ethylmorpholine (0.5 mL). Following a 16-h reflux, $AgNO_3$ (1.50 mmol) was added to the reaction mixture, and the resulting mixture was then left to reflux for an additional 1.5 h. The mixture was then cooled and preabsorbed on silica, and the solvent was removed in vacuo. The product was purified by chromatographic techniques (details specified below). The desired fraction was collected and isolated to yield a dark red fine solid.

*[Ru(**L4**)(**L10**)]NO_3 (**4**).* Chromatographic conditions: SiO_2; 9:1 CH_2Cl_2/MeOH; R_f = 0.59. Yield: 333 mg (0.28 mmol, 70.0%). ^{1}H NMR (400 MHz, $CDCl_3$): δ 9.16 (s, 2H, H_E), 9.05 (d, 1H, ^3J = 1.4 Hz, H_e), 9.02 (d, 1H, ^3J = 7.3 Hz, H_d), 8.92 (d, 2H, ^4J = 0.8 Hz, H_D), 8.25 (d, 1H, ^3J = 1.4 Hz, H_m), 8.22 (d, 1H, ^3J = 3.9 Hz, H_f), 7.93 (s, 1H, H_n), 7.92 (dt, 1H, ^3J = 7.5 Hz, ^4J = 1.0 Hz, H_c), 7.70−7.63 (m, 4H, H_A, H_B), 7.58 (d, 2H, ^3J = 8.9 Hz, H_h), 7.42 (d, 1H, ^3J = 3.9 Hz, H_g), 7.31−7.24 (m, 5H, H_a, H_k), 7.17−7.03 (m, 9H, H_b, H_i, H_j, H_l), 6.66 (d, 1H, ^3J = 7.3 Hz, H_p), 5.53 (d, 1H, ^3J = 7.6 Hz, H_q), 4.19 (s, 3H, H_F), 3.94 (s, 6H, H_C). HRMS (ESI): m/z 1133.1901 [$(M)^+$] (calcd for $C_{60}H_{42}F_3N_6O_6RuS^+$: m/z 1133.1882). Anal. Calcd for $C_{60}H_{42}F_3N_7O_9RuS\cdot 2H_2O$: C, 58.53; H, 3.77; N, 7.96. Found: C, 58.18; H, 4.10; N, 7.58.

*[Ru(**L5**)(**L10**)]NO_3 (**5**).* Chromatographic conditions: SiO_2; 9:1 CH_2Cl_2/MeOH; R_f = 0.45. Yield: 334 mg (0.28 mmol, 70.4%). ^{1}H NMR (400 MHz, $CDCl_3$): δ 9.16 (s, 2H, H_E), 9.01 (d, 1H, ^3J = 1.4 Hz, H_e), 8.99 (d, 1H, ^3J = 7.3 Hz, H_d), 8.92 (d, 2H, ^4J = 0.8 Hz, H_D), 8.24 (d, 1H, ^3J = 1.4 Hz, H_m), 8.20 (d, 1H, ^3J = 3.9 Hz, H_f), 7.96−7.88 (m, 2H, H_n, H_c), 7.70−7.65 (m, 4H, H_A, H_B), 7.54 (d, 2H, ^3J = 8.9 Hz, H_h), 7.39 (d, 1H, ^3J = 3.9 Hz, H_g), 7.27 (d, 1H, ^3J = 5.3 Hz, H_a), 7.09 (d, 4H, ^3J = 8.3 Hz, H_k), 7.12−7.00 (m, 7H, H_b, H_i, H_j), 6.66 (d, 1H, ^3J = 7.3 Hz, H_p), 5.53 (d, 1H, ^3J = 7.6 Hz, H_q), 4.19 (s, 3H, H_F), 3.94 (s, 6H, H_C), 2.32 (s, 6H, H_l). HRMS (ESI): m/z 1161.2210 [$(M)^+$] (calcd for $C_{62}H_{46}F_3N_6O_6RuS^+$: m/z 1161.2195). Anal. Calcd for $C_{62}H_{46}F_3N_7O_9RuS\cdot 2H_2O$: C, 59.14; H, 4.00; N, 7.79. Found: C, 59.13; H, 4.06; N, 7.55.

*[Ru(**L6**)(**L10**)]NO_3 (**6**).* Chromatographic conditions: SiO_2; 9:1 CH_2Cl_2/MeOH; R_f = 0.63. Yield: 306 mg (0.24 mmol, 61.2%). ^{1}H NMR (400 MHz, $CDCl_3$): δ 9.15 (s, 2H, H_E), 9.01 (d, 1H, ^3J = 1.4 Hz, H_e), 9.00 (d, 1H, ^3J = 7.3 Hz, H_d), 8.92 (d, 2H, ^4J = 0.8 Hz, H_D), 8.24 (d, 1H, ^3J = 1.4 Hz, H_m), 8.21 (d, 1H, ^3J = 3.9 Hz, H_f), 7.97−7.88 (m, 2H, H_n, H_c), 7.70−7.63 (m, 4H, H_A, H_B), 7.52 (d, 2H, ^3J = 8.9 Hz, H_h), 7.38 (d, 1H, ^3J = 3.9 Hz, H_g), 7.27 (d, 1H, ^3J = 5.3 Hz, H_a), 7.12−7.06 (m, 5H, H_k, H_b), 6.95 (d, 2H, ^3J = 8.9 Hz, H_i), 6.85 (d, 4H, ^3J = 8.2 Hz, H_j), 6.66 (d, 1H, ^3J = 7.3 Hz, H_p), 5.53 (d, 1H, ^3J = 7.6 Hz, H_q), 4.19 (s, 3H, H_F), 3.94 (s, 6H, H_C), 3.80 (s, 6H, H_l). HRMS (ESI): m/z 1193.2114 [$(M)^+$] (calcd for $C_{62}H_{46}F_3N_6O_8RuS^+$: m/z 1193.2093). Anal. Calcd for $C_{62}H_{46}F_3N_7O_{11}RuS\cdot 2H_2O$: C, 57.67; H, 3.90; N, 7.59. Found: C, 57.85; H, 4.19; N, 7.27.

*[Ru(**L7**)(**L10**)]NO_3 (**7**).* Chromatographic conditions: SiO_2; 9:1 CH_2Cl_2/MeOH; R_f = 0.56. Yield: 254 mg (0.22 mmol, 55.2%). ^{1}H NMR (400 MHz, $CDCl_3$): δ 9.10 (s, 2H, H_E), 8.92 (d, 1H, ^3J = 7.3 Hz, H_d), 8.89 (d, 1H, ^3J = 1.4 Hz, H_e), 8.87 (d, 2H, ^4J = 0.8 Hz, H_D), 8.27 (d, 1H, ^3J = 1.4 Hz, H_m), 8.17 (d, 1H, ^3J = 3.9 Hz, H_f), 7.90 (dt, 1H, ^3J = 7.6 Hz, ^4J = 1.0 Hz, H_c), 7.67 (d, 2H, ^3J = 5.4 Hz, H_A), 7.61 (dd, 2H, ^3J = 5.4 Hz, ^4J = 1.0 Hz, H_B), 7.55 (d, 2H, ^3J = 8.9 Hz, H_h), 7.54 (d, 1H, ^3J = 7.8 Hz, H_n), 7.40 (d, 1H, ^3J = 3.9 Hz, H_g), 7.28 (t, 4H, ^3J = 8.3 Hz, H_k), 7.17−7.00 (m, 9H, H_j, H_b, H_i, H_l), 6.92 (d, 1H, ^3J = 5.3 Hz, H_a), 6.81 (t, 1H, ^3J = 7.8 Hz, H_o), 5.97 (d, 1H, ^3J = 7.8 Hz, H_p), 4.19 (s, 3H, H_F), 3.94 (s, 6H, H_C), 2.74 (s, 3H, H_q). HRMS (ESI): m/z 1095.2125 [$(M)^+$] (calcd for $C_{60}H_{45}N_6O_7RuS^+$: m/z 1095.2114). Anal. Calcd for $C_{60}H_{45}N_7O_{10}RuS\cdot 2H_2O$: C, 60.40; H, 4.14; N, 8.22. Found: C, 60.68; H, 4.24; N, 7.83.

*[Ru(**L8**)(**L10**)]NO_3 (**8**).* Chromatographic conditions: SiO_2; 9:1 CH_2Cl_2/MeOH; R_f = 0.61. Yield: 313 mg (0.26 mmol, 66.4%). ^{1}H NMR (400 MHz,

$CDCl_3$): δ 9.10 (s, 2H, H_E), 8.90 (d, 1H, ^3J = 7.3 Hz, H_d), 8.87 (m, 3H, H_e, H_D), 8.27 (d, 1H, ^3J = 1.4 Hz, H_m), 8.16 (d, 1H, ^3J = 3.9 Hz, H_f), 7.91 (dt, 1H, ^3J = 7.6 Hz, ^4J = 1.0 Hz, H_c), 7.66 (d, 2H, ^3J = 5.4 Hz, H_A), 7.61 (dd, 2H, ^3J = 5.4 Hz, ^4J = 1.0 Hz, H_B), 7.54 (d, 1H, ^3J = 7.8 Hz, H_n), 7.51 (d, 2H, ^3J = 8.9 Hz, H_h), 7.38 (d, 1H, ^3J = 3.9 Hz, H_g), 7.09 (d, 4H, ^3J = 8.3 Hz, H_k), 7.06−7.00 (m, 7H, H_j, H_b, H_i), 6.93 (d, 1H, ^3J = 5.3 Hz, H_a), 6.81 (t, 1H, ^3J = 7.8 Hz, H_o), 5.97 (d, 1H, ^3J = 7.8 Hz, H_p), 4.19 (s, 3H, H_F), 3.94 (s, 6H, H_C), 2.74 (s, 3H, H_q), 2.32 (s, 6H, H_l). HRMS (ESI): m/z 1123.2434 [$(M)^+$] (calcd for $C_{62}H_{49}N_6O_7RuS^+$: m/z 1123.2427). Anal. Calcd for $C_{62}H_{49}N_7O_{10}RuS\cdot 2H_2O$: C, 60.98; H, 4.37; N, 8.03. Found: C, 60.76; H, 4.51; N, 7.69.

*[Ru(**L9**)(**L10**)]NO_3 (**9**).* Chromatographic conditions: SiO_2; 9:1 CH_2Cl_2/MeOH; R_f = 0.58. Yield: 356 mg (0.29 mmol, 73.5%). ^{1}H NMR (400 MHz, $CDCl_3$): δ 9.10 (s, 2H, H_E), 8.87 (s, 2H, H_D), 8.86 (d, 1H, ^3J = 7.3 Hz, H_d), 8.83 (d, 1H, ^3J = 1.4 Hz, H_e), 8.26 (d, 1H, ^3J = 1.4 Hz, H_m), 8.13 (d, 1H, ^3J = 3.9 Hz, H_f), 7.90 (dt, 1H, ^3J = 7.6 Hz, ^4J = 1.0 Hz, H_c), 7.66 (d, 2H, ^3J = 5.4 Hz, H_A), 7.61 (dd, 2H, ^3J = 5.4 Hz, ^4J = 1.0 Hz, H_B), 7.54 (d, 1H, ^3J = 7.8 Hz, H_n), 7.48 (d, 2H, ^3J = 8.9 Hz, H_h), 7.35 (d, 1H, ^3J = 3.9 Hz, H_g), 7.09 (d, 4H, ^3J = 8.3 Hz, H_k), 7.03 (dt, 1H, ^3J = 7.6 Hz, ^4J = 1.0 Hz, H_b), 6.93 (d, 3H, ^3J = 8.9 Hz, H_i, H_a), 6.85 (d, 4H, ^3J = 8.2 Hz, H_j), 6.80 (t, 1H, ^3J = 7.8 Hz, H_o), 5.97 (d, 1H, ^3J = 7.8 Hz, H_p), 4.19 (s, 3H, H_F), 3.94 (s, 6H, H_C), 3.79 (s, 6H, H_l), 2.74 (s, 3H, H_q). HRMS (ESI): m/z 1155.2327 [$(M)^+$] (calcd for $C_{62}H_{49}N_6O_9RuS^+$: m/z 1155.2325). Anal. Calcd for $C_{62}H_{49}N_7O_{12}RuS\cdot 2H_2O$: C, 59.42; H, 4.26; N, 7.82. Found: C, 59.03; H, 4.39; N, 7.44.

*[Ru(**pbpy**)(**L10**)]NO_3 (**10**).* Chromatographic conditions: SiO_2; 9:1 CH_2Cl_2/MeOH; R_f = 0.50. Yield: 148 mg (0.19 mmol, 46.4%). ^{1}H NMR (400 MHz, $CDCl_3$): δ 9.13 (s, 2H, H_E), 8.90 (s, 2H, H_D), 8.74 (d, 1H, ^3J = 8.0 Hz, H_e), 8.70 (d, 1H, ^3J = 8.0 Hz, H_d), 8.23 (t, 1H, ^3J = 8.0 Hz, H_s), 8.14 (d, 1H, ^3J = 8.0 Hz, H_m), 7.90 (dt, 1H, ^3J = 8.0 Hz, ^4J = 1.2 Hz, H_c), 7.70 (d, 1H, ^3J = 7.6 Hz, H_a), 7.67−7.63 (m, 4H, H_A, H_B), 7.17 (d, 1H, ^3J = 4.8 Hz, H_n), 7.03 (t, 1H, ^3J = 7.2 Hz, H_b), 6.74 (t, 1H, ^3J = 7.6 Hz, H_p), 6.44 (t, 1H, ^3J = 7.8 Hz, H_o), 5.33 (d, 1H, ^3J = 7.2 Hz, H_q), 4.19 (s, 3H, H_F), 3.94 (s, 6H, H_C). HRMS (ESI): m/z 740.1087 [$(M)^+$] (calcd for $C_{37}H_{28}N_5O_6Ru^+$: m/z 740.1083). Anal. Calcd for $C_{37}H_{28}N_6O_9Ru\cdot H_2O$: C, 54.21; H, 3.69; N, 10.25. Found: C, 54.56; H, 3.92; N, 9.88.

Physical Methods. Elemental analysis (EA), electrospray ionization mass spectrometry (ESI-MS), matrix-assisted laser desorption/ionization mass spectrometry (MALDI-TOF), and electron impact (EI) mass spectrometry data were collected at the Chemistry Instrumentation Facility of the University of Calgary. Electrochemical measurements were performed under anaerobic conditions with a Princeton Applied Research VersaStat 3 potentiostat using dry solvents, platinum working and counter electrodes, a silver pseudoreference electrode, and a 0.1 M NBu_4BF_4 supporting electrolyte. Electronic spectroscopic data were collected on MeOH solutions using a Cary 5000 UV−vis spectrophotometer (Varian). Steady-state emission spectra were obtained at room temperature using an Edinburgh Instruments FLS920 spectrometer equipped with a Xe900 450-W steady-state xenon arc lamp, a TMS300-X excitation monochromator, a TMS300-M emission monochromator, and a Hamamatsu R2658P PMT detector and corrected for detector response. Lifetime measurements were obtained at room temperature using an Edinburgh Instruments FLS920 spectrometer equipped with a Fianium SC400 super continuum white light source and a Hamamatsu R3809U-50 multichannel plate detector, and data were analyzed with Edinbrugh Instruments F900 software. Curve fitting of the data was performed using a nonlinear least-squares procedure in the F900 software.

Computational Methods. The *Gaussian 03* computational package[62] to perform ground-state geometry optimization calculations employing Becke's three-parameter hybrid exchange functional, the Lee−Yang−Parr non-local correlation functional B3LYP,[63,64] and SDD basis set[65,66] with an effective core potential, was used for the Ru atom and a 6-31G* basis set was used for C, H, N, P, and Cl atoms.[67] Time-dependent density functional theory (TDDFT) calculations were also performed using this methodology, and the first 60 singlet excited states were calculated. Calculations by the first-principles method were used to obtain accurate excitation energies and oscillator strengths. We modeled the solvent with the polarizable continuum model using MeOH as the solvent.[68,69]

RESULTS AND DISCUSSION

Synthesis and Structural Characterization. A modular synthetic approach (Scheme 1) was used to isolate the library of TPA-functionalized tridentate ligands in Chart 1. The synthesis of each of these donor ligands was achieved in reasonably high yield on a large scale utilizing well-established synthetic methods. Proligands **P4**−**P6** were synthesized through Kröhnke condensations to yield the bromothiophene-substituted pbpy platform, which were further reacted with Suzuki reagents (e.g., **P1**−**P3**) to give the desired ligands, **L1H**−**L9H**, in high yields.

Following previously established synthetic routes,[5,10] the syntheses of the cyclometalated complexes were achieved through reaction of the Ru(**L10**)Cl_3 synthon with the corresponding ligand, producing the methyl ester complexes (**1**−**9**) in high yields ranging between 55 and 70% after chromatographic purification to remove the byproduct (Scheme S1 in the Supporting Information). The structural identities of all ligands and complexes were confirmed by a combination of NMR spectroscopy, mass spectrometry, and/or EA. ^{1}H NMR (1D and 2D) spectroscopy is a particularly effective diagnostic tool for these complexes because of separation of the aromatic signals and the inherent asymmetry of the complexes. A collection of representative ^{1}H NMR spectra are provided in Figure 2 to illustrate the effect of substitution on the anionic ring of the pbpy chelate with EWGs or EDGs (e.g., **2**, **5**, and **8**). A signature of cyclometalation of the TPA-substituted pbpy ligand is the upfield shift of the signal corresponding to the proton ortho to the Ru−C bond (i.e., H_q) that arises because of the proximity of the anionic carbon. This signal is observed for compounds with either −H (e.g., **2**) or $-CF_3$ (e.g., **5**) on the anionic ring (Figure 2). The electron-withdrawing nature of the $-CF_3$ group is revealed in the downfield chemical shift of the proton ortho to the Ru−C bond, H_q, of **5** (H_q = 5.53 ppm) relative to the −H-substituted analogue **2** (H_q = 5.35 ppm). Curiously, the most-upfield signal in the aromatic region for −OMe-substituted complex **8** is not H_q but is instead a doublet corresponding to the resonance signal of the proton meta to the Ru−C bond, H_p, at 5.97 ppm. This signature provides direct evidence that the −OMe group appears at the R_3 position (i.e., ortho to the Ru−C bond) rather than at the R_2 position (vide infra). Because the position of the substituent on the phenyl ring of the pbpy chelate is found to fluctuate in the series (i.e., at either R_2 or R_3), H_n emerges as a better spectroscopic handle to probe the electronic effects of substitution for this particular series. In this regard, the chemical shift of H_p follows the expected trend of electron density on the anionic ring, e.g., **2** (6.47 ppm), **5** (6.66 ppm), and **8** (5.97 ppm).

C−H activation takes place para to the substituent on the anionic ring for the complexes bearing $-CF_3$ substituents anionic (e.g., **5**). Taking into account the electron-withdrawing character of the $-CF_3$ group, it is not remarkable that the C−H bond para to the substituent is activated to form the Ru−C bond.

Scheme 1. Synthesis of Precursors P4−P6 and Ligands L1H−L9H[a]

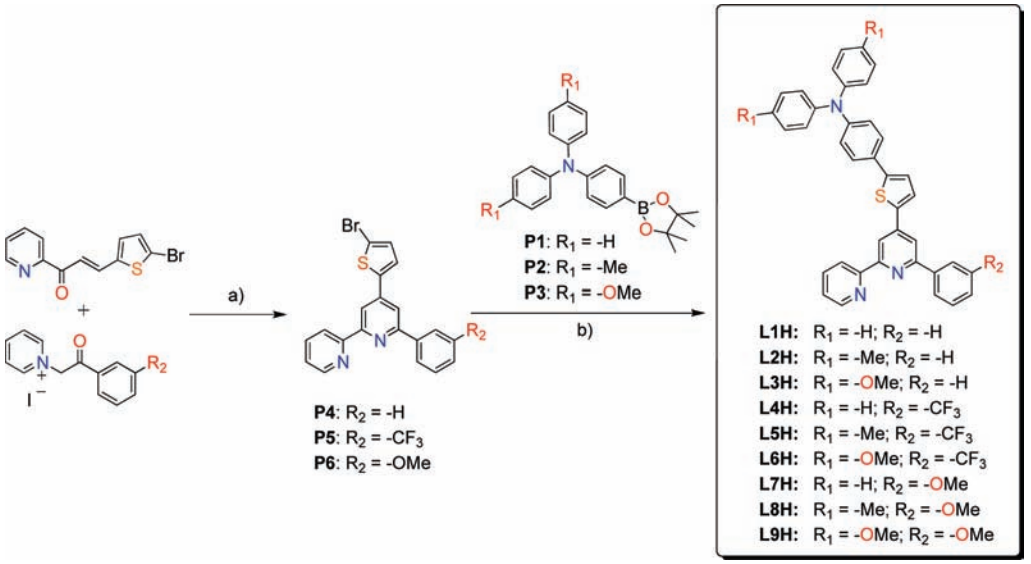

[a] Reaction conditions: (a) ammonium acetate, formamide, 120 °C, 14 h; (b) $Pd(PPh_3)_4$, K_2CO_3, THF/H_2O (9:1); 65 °C, 14 h.

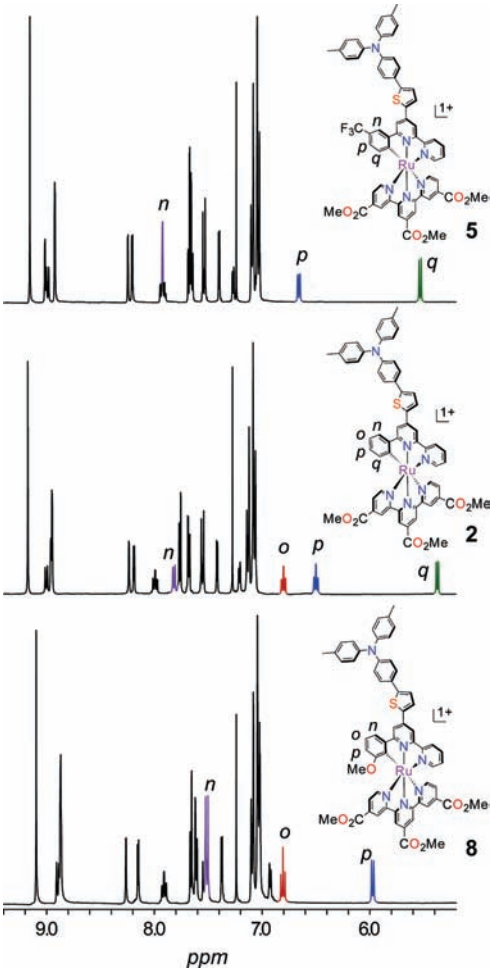

Figure 2. ^1H NMR spectra for $CDCl_3$ solutions of **5**, **2**, and **8** at ambient temperatures highlighting how substituents affect the electron density on the anionic ring. Color scheme: green, H_q; red, H_s; blue, H_p; purple, H_n.

We anticipated that the −OMe substituent would also appear para to the Ru−C bond due to steric considerations; however, the C−H activation step is found to occur ortho to the −OMe group. It appears that this anomaly is a result of the more thermodynamically stable isomer being the favored product. This hypothesis is corroborated by electrochemical data that indicate that this isomer is more stable by ∼130 mV (vide infra).

Electrochemical Data. The electrochemical properties of the free ligands and the corresponding metal complexes were examined in CH_2Cl_2 by cyclic voltammetry. Relevant redox values are collected in Table 1. The redox properties of similar TPA-substituted ligands have been discussed previously.[10,48] In brief, there is a single quasi-reversible one-electron oxidation ($E_{1/2}^{ox}$ = +0.98−1.22 V) localized to the TPA portion of the ligand (i.e., $TPA^{\bullet+}/TPA^0$). The position of this oxidation wave remains static after coordination to the ruthenium metal (Figure 3); however, it is sensitive to the solvent medium (e.g., the $TPA^{\bullet+}/TPA^0$ oxidation potential is shifted ∼−70 mV in MeCN).

An anodic sweep of each of the solutions containing the cyclometalated complexes typically produces two consecutive quasi-reversible single-electron oxidation processes that correspond to oxidation of the TPA unit and ruthenium(II) metal; the differences in $E_{p,a}$ and $E_{p,c}$ (i.e., ΔE) are provided in Table 1. The careful assignment of the oxidative behavior was aided by references to previously reported compounds;[10] however, in certain cases, differential pulse voltammetry (DPV) was required to resolve the closely spaced oxidation processes (e.g., **1**, **2**, **7**, and **8**). As stated above, the $TPA^{\bullet+}/TPA^0$ oxidation potential is not affected by ligation to the {Ru(**L10**)} core, nor is it affected by substitution of the pbpy chelate; i.e., the oxidation potential is the same for the free ligand and complex [e.g., ∼+1.2 V for **L1H** and **1**, ∼+1.1 V for **L5H** and **5** (Figure 3), and ∼+1.0 V for **L9H** and **9**]. Similarly, the Ru^{III}/Ru^{II} redox couple is not affected by substitution of TPA at R_1 (e.g., +1.17 V for **1**−**3**, respectively). With installation of the $-CF_3$ group at the R_2 position, the Ru^{III}/Ru^{II} redox couple resides at +1.27 V, which is +100 and +170 mV greater than the cases where R_2 = −H and R_3 = −OMe, respectively. Note that a −OMe substitutent para to the Ru−C bond can

dx.doi.org/10.1021/ic1025679 |Inorg. Chem. 2011, 50, 6019–6028

Table 1. Summary of the Spectroscopic and Electrochemical Properties for Ligands L1H−L9H and Complexes 1−10

		emission data[b]		$E_{1/2}$, V vs NHE[d]	
compound	UV−vis absorbance data:[a] λ_{max}, nm ($\varepsilon \times 10^3$, $M^{-1}\cdot cm^{-1}$)	λ_{em}, nm	τ, ns;[c] φ	Ru^{III}/Ru^{II}	$TPA^{\bullet+}/TPA^0$
L1H	391 (26.7)	536 (390)	3.4 (0.99); 0.91	[e]	1.20
1	681^{sh} (3.4), 584^{sh}, 526 (26.7), 431 (39.4), 330 (42.4)	549 (429)	3.2 (1.02); 0.27	1.17 (72) [f]	1.21 (75) [f]
L2H	399 (31.2)	563 (397)	3.8 (1.04); 0.58	[e]	1.10
2	681^{sh} (3.5), 584^{sh}, 526 (28.4), 435 (39.3), 330 (42.5)	561 (433)	3.6 (1.00); 0.24	1.17 (87) [g]	1.11 (89) [g]
L3H	404 (33.2)	616 (401)	0.6 (0.91); 0.16	[e]	0.99
3	681^{sh} (2.9), 574^{sh}, 527 (29.6), 437 (37.5), 331 (41.0)	[e]	[e]	1.17 (86)	0.99 (89)
L4H	420 (23.8)	545 (391)	3.3 (0.94); 0.81	[e]	1.20
4	664^{sh} (4.0), 572^{sh}, 517 (33.0), 427 (43.1), 328 (50.7)	[e]	[e]	1.27 (91) [h]	1.19 (92) [h]
L5H	402 (29.0)	573 (419)	3.4 (1.06); 0.52	[e]	1.11
5	666^{sh} (4.2), 571^{sh}, 518 (37.6), 430 (44.1), 329 (54.3)	[e]	[e]	1.27 (80)	1.10 (78)
L6H	408 (25.0)	632 (403)	0.5 (0.97); 0.34	[e]	0.99
6	666^{sh} (4.1), 571^{sh}, 520 (39.1), 431 (41.5), 330 (52.6)	[e]	[e]	1.27 (93)	0.98 (96)
L7H	391 (28.4)	535 (387)	2.9 (0.96); 0.55	[e]	1.20
7	664^{sh} (4.3), 571^{sh}, 531 (29.1), 433 (45.9), 329 (51.2)	[e]	[e]	1.11 (76)	1.20 (74)
L8H	399 (31.2)	563 (396)	4.0 (1.09); 0.82	[e]	1.10
8	667^{sh} (4.0), 571^{sh}, 532 (29.2), 437 (43.4), 330 (48.6)	[e]	[e]	1.09 (77)	1.09 (77)
L9H	404 (33.5)	621 (401)	[e]; 0.18	[e]	0.98
9	668^{sh} (4.2), 571^{sh}, 532 (32.8), 439 (44.9), 330 (50.8)	[e]	[e]	1.10 (88)	0.98 (90)
10[i]	684^{sh} (3.0), 574^{sh}, 523 (9.7), 433 (17.0), 329 (29.6)	[e]	[e]	1.12	[e]

[a] Data collected in MeOH. [b] Data collected in MeCN; λ_{ex} values indicated in parentheses with units of nm. [c] χ^2 indicated in parentheses; absolute quantum yield measured with an integrating sphere. [d] Data collected using 0.1 M NBu_4BF_4/CH_2Cl_2 solutions at 100 mV/s and referenced to a $[Fc]/[Fc]^+$ or $[OFc]/[OFc]^+$ internal standard followed by conversion to NHE; $[Fc]/[Fc^+] = +765$ mV vs NHE in CH_2Cl_2; $[OFc]/[OFc]^+ = +290$ mV vs NHE in CH_2Cl_2; values in parentheses are the ΔE values of $E_{p,a}$ and $E_{p,c}$ given in mV determined from DPV experiments. [e] Not observed. [f] Oxidative sweep in DPV experiments produces two peaks resolved by 40 mV. [g] Oxidative sweep generates two peaks resolved by 60 mV in DPV experiments. [h] Oxidative sweep generates two peaks resolved by 80 mV in DPV experiments. [i] Benchmark complex: [Ru(pbpy)(**L10**)](NO_3). Superscript "sh" indicates shoulder.

lower the Ru^{III}/Ru^{II} oxidation potential by ca. ~200 mV;[28] thus, the observation that this couple is only affected by ~70 mV is primarily attributed to the −OMe substituent being positioned ortho to the Ru−C bond. The stabilizing effect of this EDG ortho to the organometallic bond (rather than para) is rationalized by the suppressed donating ability of the O-atom lone-pair into the aromatic ring due to hindered steric rotation about the C−OMe bond.

Optical Properties. Electronic absorption and emission data were collected to delineate the effects of substitution at the R_1 and R_2/R_3 positions (Table 1). Each of the free TPA-substituted ligands displays a relatively broad intense absorption band centered within the 390−420 nm range (Figure S2 in the Supporting Information) that arises from a series of intramolecular $\pi \rightarrow \pi^*$ transitions emanating from the TPA fragment to the π^* system of the pbpy fragment. Ligation to the metal center renders a broad and intense absorption envelope for each of the complexes due to multiple intraligand charge-transfer (ILCT) and metal-to-ligand charge-transfer (MLCT) transitions (Figure 4).

A general assignment of the principle electronic transitions for the title complexes is made possible by the extensive library of related compounds available to us within this study as well as our prior work.[10] The optical spectra for **1**−**3** in Figure 4a show that there are negligible changes in the intensities and positions of the absorption spectra when different substituents are installed at the R_1 position. The slight increase in the extinction coefficient at ~540 nm for complex **3** is ascribed to a higher transition dipole induced by the electron-rich −OMe substituent on the TPA unit. Figure 4b reveals a slightly more pronounced effect on the optical properties when the pbpy chelate is modified. The position of the lowest-energy maxima reflects a higher metal-based HOMO level (involving the d_{xy} orbital) with progressively greater electron density on the anionic ring; e.g., λ_{max} follows the trend **8** (532 nm) > **2** (526 nm) > **5** (518 nm). This trend is also consistent with the lowest-energy absorption band containing a significant MLCT contribution emanating from the occupied d_{xy} orbital to the π^* orbital of the **L10** ligand (vide infra). There are, however, ILCT contributions within the low-energy band, as evidenced by the slightly lower shoulder at ca. 570 nm that becomes more prominent with substituents on the pbpy chelate. In the case of **5**, for example, there appears to be an enhancement of the transition dipole for the ILCT transition furnished by the electron-deficient CF_3-substituted pbpy chelate (i.e., from $\pi_{TPA} \rightarrow \pi^*$ of the pbpy chelate). Consequently, the most intense low-energy band is observed for **5**, followed by **2** and **3**, respectively.

DFT. Ground-state optimization and TDDFT calculations were performed to aid the assignment of the optical spectra. The four major predicted transitions and the corresponding molecular orbital diagrams are shown for **1** in Figure 5. The lowest-energy transition, λ_1, involves a transition from the HOMO−1 orbital containing significant Ru d_{xy} character to the LUMO, which contains π^*-orbital character over the Me_3tctpy ligand. We note that the shoulder may also have some contribution from the direct population of a ^{3}MLCT state facilitated by the heavy-metal ion.[70] The transition λ_2 at 599 nm contains two transitions of approximately equal weight (i.e., HOMO−1 → LUMO+1 and

dx.doi.org/10.1021/ic1025679 |*Inorg. Chem.* 2011, 50, 6019–6028

HOMO−2 → LUMO). The orbital character for the HOMO−2 is distributed over the Ru d_{xz} orbital and the π system extending over the thiophene spacer and TPA; the LUMO and LUMO+1 orbitals are both localized over the π^* system of the anchoring Me_3tctpy ligand. The orbital character for the HOMO−3 orbital, which is involved in λ_4, is primarily Ru d_{yz} in character, with some minor contributions from the π system of the anionic portion of the cyclometalating ring and the Me_3tctpy ligand. The spectral analysis for **2**−**9** is provided as Supporting Information (Figures S3−S10). In general, the first three low-energy transitions (λ_1−λ_3) involve the promotion of electrons from molecular orbitals localized over TPA and/or the ruthenium metal and anionic ring to the π^* system of the Me_3tctpy ligand. The highest-energy transition (i.e., λ_4) involves a filled orbital with character that is either localized to the TPA or over the d_{yz} orbital. We note that all four light-induced transitions λ_1−λ_4 involve the movement of electron density toward Me_3tctpy, which is ideal for sensitization applications.

The predicted UV−vis spectra match well with the experimental spectra; indeed, the oscillator strengths of the calculated transitions match well with the molar extinction coefficients derived from experiment. One curious result, however, is the prediction that the HOMO resides on the TPA in all cases. This finding contrasts the electrochemical data, which clearly indicate that the first oxidation potential is not always TPA-based (e.g., **1** and **7**). We ascribe this discrepancy to solvation of the TPA unit: the oxidation potential of the $TPA^{\bullet+}/TPA^0$ couple can shift to more positive values in polar solvents (e.g, a ∼−70 mV shift when the solvent is switched from CH_2Cl_2 to MeCN). Thus, in the absence of an appropriate solvation model for the TPA unit, we anticipate the predicted thermodynamic position of the HOMO localized to TPA to be shifted to more negative values.

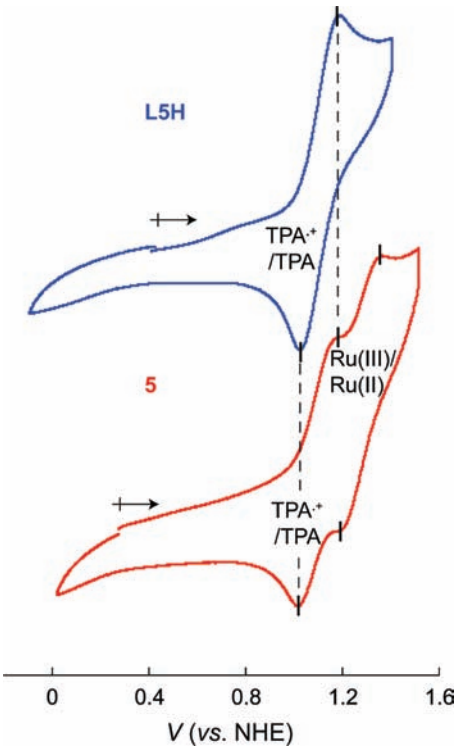

Figure 3. Cyclic voltammograms for ligand **L5H** and the corresponding metal complex **5** in CH_2Cl_2 at ambient temperatures (scan rate = 100 mV/s). Dashed lines emphasize that $E_{p,a}$ and $E_{p,c}$ of the $TPA^{\bullet+}/TPA^0$ couple are the same as those for the free ligand and complex.

SUMMARY

The primary objective of this synthetic endeavor is to develop a series of complexes where a direct correlation of the properties to the molecular structure could be established to guide the design of cyclometalated complexes for light-harvesting applications. Building on our previous studies,[10,48] we have expanded the development of the dual-chromophore scaffold, [Ru(TPA-pbpy)(Me_3tctpy)], to show that we can systematically tune the electrochemical behavior of *both* the ruthenium and TPA units. We show that the electronic properties of each electrophore can be manipulated to make the Ru^{III}/Ru^{II} couple more or less oxidizing than the TPA unit. This feature is possible because the ground-state oxidation potentials of the each unit can be modulated over a wide range of potentials: $\Delta E_{1/2}$ = 180 and 230 mV for the Ru^{III}/Ru^{II} and $TPA^{\bullet+}/TPA$ couples, respectively. Consequently, the HOMO character can be positioned on either the metal chelate or the TPA unit, with the latter scenario being optimal for sensitizing TiO_2.[10,47,51]

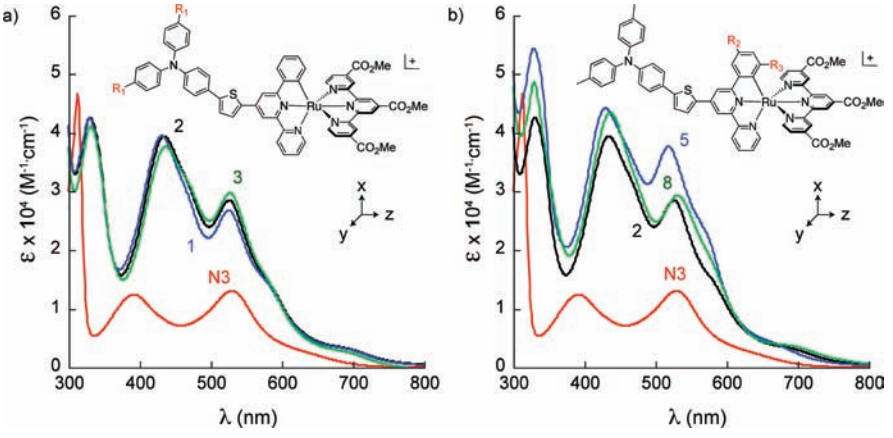

Figure 4. UV−vis absorption spectra demonstrating the (a) minor optical changes when R_1 = −H (**1**), −Me (**2**), and −OMe (**3**) and (b) the more significant optical response to substituents at the pbpy chelate (e.g., **2**, R_2/R_3 = −H; **5**, R_2 = $-CF_3$, R_3 = −H; **8**, R_2 = −H, R_3 = −OMe). The spectrum of **N3** is also provided as a benchmark.

dx.doi.org/10.1021/ic1025679 |*Inorg. Chem.* 2011, 50, 6019–6028

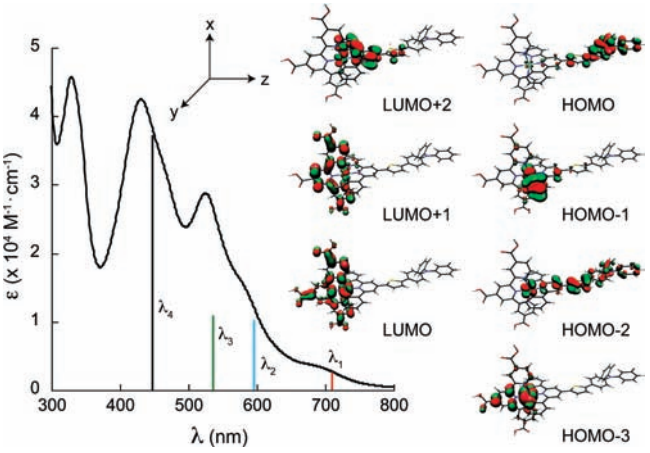

Figure 5. Experimental UV−vis absorption spectrum of **1** overlaid with calculated transitions represented by vertical bars (only the transitions with contributions >40% are shown). Details of calculated transitions (theoretical wavelength in nm, oscillator strength, % contribution to the transition): λ_1, HOMO−1 → LUMO (709, 0.027, 85%); λ_2, HOMO−2 → LUMO (594, 0.11, 50%) and HOMO−1 → LUMO+1 (594, 0.11, 40%); λ_3, HOMO−2 → LUMO+1 (536, 0.11, 85%); λ_4, HOMO−3 → LUMO+2 (447, 0.38, 64%).

In contrast to the rich electrochemical behavior, the relative positions of the two redox units are found to have negligible effects on the optical properties: substitution at both the R_1 and R_2/R_3 positions produces minor changes in both the intensities and shapes of the absorbance profiles. This finding stands in stark contrast to the significant spectral changes that occur when the position of the organometallic bond in this platform is varied.[10] Notwithstanding, the differences in the optical spectra, however slight, remain consistent with the dipole changes—and relative weighting—for both the ILCT and MLCT transitions and harvest a significant amount of light out to 800 nm (note that the optical profiles are superior to that of **N3;** Figure 4). Thus, the ability to control the redox properties without affecting the optical properties provides a distinct advantage for inducing an electronic cascade and the thermodynamic driving force for the reaction between the electrolyte and photooxidized dye. Transient spectroscopic studies are underway to further unravel the electron-transfer events that occur after light absorption.

This work adds further evidence that bichromic cyclometalated ruthenium(II) complexes offer a number of benefits over tridentate polypyridylruthenium(II) compounds for sensitizing TiO_2. Distortion of the ligand field by the anionic cyclometalating ligands leads to a broad absorption envelope while increasing the π^* orbital of the LUMO, which will presumably lead to enhanced rates of electron injection into the TiO_2 anode.[71] The incorporation of a secondary chromophore is shown to increase the intensity of the absorption bands substantially compared to analogous tridentate cyclometalated derivatives.[28] Moreover, previous studies have shown that the TPA unit can increase the excited-state lifetime of the ruthenium chromophore and spatial charge separation on TiO_2.[47,50,52,72] The device performance for this entire suite of complexes in liquid-junction and solid-state DSSCs will be disseminated in a future study.

■ ASSOCIATED CONTENT

Ⓢ Supporting Information. UV−vis absorption spectra highlighting the optical affects of the position of the Ru−C bond and ligands **L1H**−**L9H** in MeOH, a synthetic scheme for compounds **1**−**9**, comparative ^{1}H NMR spectra for **2**, **5**, and **8**, and molecular orbital pictures and TDDFT spectra for **2**−**9**. This material is available free of charge via the Internet at http://pubs.acs.org.

■ AUTHOR INFORMATION

Corresponding Author
*E-mail: cberling@ucalgary.ca.

■ ACKNOWLEDGMENT

This work was financially supported by the Canadian Natural Science and Engineering Research Council (NSERC), Canada Research Chairs, Canadian Foundation for Innovation (CFI), Alberta Ingenuity, and the Canada School of Energy and Environment (CSEE). We are also grateful to NSERC (K.C.D. R., B.S., and E.S.), Alberta Innovates (K.C.D.R.), and DI-26-10/I, AT24100024, and CONICYT (E.S.) for student fellowships.

■ REFERENCES

(1) O'Regan, B.; Grätzel, M. *Nature* **1991**, *353*, 737–740.
(2) Hagfeldt, A.; Boschloo, G.; Sun, L.; Kloo, L.; Pettersson, H. *Chem. Rev.* **2010**, *110*, 6595–6663.
(3) Wadman, S. H.; Kroon, J. M.; Bakker, K.; Lutz, M.; Spek, A. L.; van Klink, G. P. M.; van Koten, G. *Chem. Commun.* **2007**, 1907–1909.
(4) Bessho, T.; Yoneda, E.; Yum, J.-H.; Guglielmi, M.; Tavernelli, I.; Imai, H.; Rothlisberger, U.; Nazeeruddin, M. K.; Grätzel, M. *J. Am. Chem. Soc.* **2009**, *131*, 5930–5934.
(5) Bomben, P. G.; Robson, K. C. D.; Sedach, P. A.; Berlinguette, C. P. *Inorg. Chem.* **2009**, *48*, 9631–9643.
(6) Funaki, T.; Yanagida, M.; Onozawa-Komatsuzaki, N.; Kasuga, K.; Kawanishi, Y.; Kurashige, M.; Sayama, K.; Sugihara, H. *Inorg. Chem. Commun.* **2009**, *12*, 842–845.
(7) Bomben, P. G.; Thériault, K. D.; Berlinguette, C. P. *Eur. J. Inorg. Chem.* **2011**, *2011*, 1806–1814.
(8) Nazeeruddin, M. K.; Kay, A.; Rodicio, I.; Humphry-Baker, R.; Müeller, E.; Liska, P.; Vlachopoulos, N.; Grätzel, M. *J. Am. Chem. Soc.* **1993**, *115*, 6382–6390.
(9) Asghar, M. I.; Miettunen, K.; Halme, J.; Vahermaa, P.; Toivola, M.; Aitola, K.; Lund, P. *Energy Environ. Sci.* **2010**, *3*, 418–426.
(10) Robson, K. C. D.; Sporinova, B.; Koivisto, B. D.; Baumgartner, T.; Yella, A.; Nazeeruddin, K. M.; Grätzel, M.; Berlinguette, C. P. *Inorg. Chem.* **2011** *50*, 5494–5508.
(11) Dixon, I. M.; Alary, F.; Heully, J.-L. *Dalton Trans.* **2010**, *39*, 10959–10966.
(12) Jacko, A. C.; McKenzie, R. H.; Powell, B. J. *J. Mater. Chem.* **2010**, *20*, 10301–10307.
(13) Jäger, M.; Smeigh, A.; Lombeck, F.; Görls, H.; Collin, J.-P.; Sauvage, J.-P.; Hammarström, L.; Johansson, O. *Inorg. Chem.* **2010**, *49*, 374–376.
(14) Wadman, S. H.; Kroon, J. M.; Bakker, K.; Havenith, R. W. A.; van Klink, G. P. M.; van Koten, G. *Organometallics* **2010**, *29*, 1569–1579.
(15) Wadman, S. H.; Lutz, M.; Tooke, D. M.; Spek, A. L.; Hartl, F.; Havenith, R. W. A.; van Klink, G. P. M.; van Koten, G. *Inorg. Chem.* **2009**, *48*, 1887–1900.
(16) Wu, K.-L.; Hsu, H.-C.; Chen, K.; Chi, Y.; Chung, M.-W.; Liu, W.-H.; Chou, P.-T. *Chem. Commun.* **2010**, *46*, 5124–5126.
(17) Collin, J. P.; Kayhanian, R.; Sauvage, J. P.; Calogero, G.; Barigelletti, F.; DeCian, A.; Fischer, J. *Chem. Commun.* **1997**, 775–776.
(18) Alonso-Vante, N.; Nierengarten, J.-F.; Sauvage, J.-P. *J. Chem. Soc., Dalton Trans.* **1994**, 1649–1654.
(19) Beley, M.; Chodorowski, S.; Collin, J.-P.; Sauvage, J.-P.; Flamigni, L.; Barigelletti, F. *Inorg. Chem.* **1994**, *33*, 2543–2547.

(20) Barigelletti, F.; Flamigni, L.; Guardigli, M.; Juris, A.; Beley, M.; Chodorowski-Kimmes, S.; Collin, J.-P.; Sauvage, J.-P. *Inorg. Chem.* **1996**, *35*, 136–142.
(21) Börgstrom, M.; Ott, S.; Lomoth, R.; Bergquist, J.; Hammarström, L.; Johansson, O. *Inorg. Chem.* **2006**, *45*, 4820–4829.
(22) Ott, S.; Borgström, M.; Hammarström, L.; Johansson, O. *Dalton Trans* **2006**, 1434–1443.
(23) Dixon, I. M.; Collin, J. P. *J. Porphyrins Phthalocyanines* **2001**, *5*, 600–607.
(24) Yam, V. W.-W.; Chu, B. W.-K.; Ko, C. C.; Cheung, K. K. *J. Chem. Soc., Dalton Trans.* **2001**, 1911–1919.
(25) Maestri, M.; Balzani, V.; Deuschel-Cornioley, C.; Von Zelewsky, A. *Adv. Photochem.* **1992**, *17*, 1–68.
(26) Djukic, J. P.; Sortais, J. B.; Barloy, L.; Pfeffer, M. *Eur. J. Inorg. Chem.* **2009**, 817–853.
(27) Constable, E. C.; Housecroft, C. E. *Polyhedron* **1990**, *9*, 1939–1947.
(28) Koivisto, B. D.; Robson, K. C. D.; Berlinguette, C. P. *Inorg. Chem.* **2009**, *48*, 9644–9652.
(29) Yao, C.-J.; Sui, L.-Z.; Xie, H.-Y.; Xiao, W.-J.; Zhong, Y.-W.; Yao, J. *Inorg. Chem.* **2010**, *49*, 8347–8350.
(30) Guillon, T.; Boggio-Pasqua, M.; Alary, F.; Heully, J.-L.; Lebon, E.; Sutra, P.; Igau, A. *Inorg. Chem.* **2010**, *49*, 8862–8872.
(31) Moorlag, C.; Sarkar, B.; Sanrame, C. N.; Bäuerle, P.; Kaim, W.; Wolf, M. O. *Inorg. Chem.* **2006**, *45*, 7044–7046.
(32) Sun, Y.; El Ojaimi, M.; Hammitt, R.; Thummel, R. P.; Turro, C. *J. Phys. Chem. B* **2010**, *114*, 14664–14670.
(33) Ardo, S.; Meyer, G. J. *Chem. Soc. Rev.* **2009**, *38*, 115–164.
(34) Durrant, J. R.; Haque, S. A.; Palomares, E. *Coord. Chem. Rev.* **2004**, *248*, 1247–1257.
(35) Kuciauskas, D.; Monat, J. E.; Villahermosa, R.; Gray, H. B.; Lewis, N. S.; McCusker, J. K. *J. Phys. Chem. B* **2002**, *106*, 9347–9358.
(36) Bomben, P. G.; Koivisto, B. D.; Berlinguette, C. P. *Inorg. Chem.* **2010**, *49*, 4960–4971.
(37) Robertson, N. *Angew. Chem., Int. Ed.* **2006**, *45*, 2338–2345.
(38) Garcia, C. G.; De Lima, J. F.; Iha, N. Y. M. *Coord. Chem. Rev.* **2000**, *196*, 219–247.
(39) Gao, F. F.; Wang, Y.; Zhang, J.; Shi, D.; Wang, M. K.; Humphry-Baker, R.; Wang, P.; Zakeeruddin, S. M.; Grätzel, M. *Chem. Commun.* **2008**, 2635–2637.
(40) Yum, J.-H.; Jung, I.; Baik, C.; Ko, J.; Nazeeruddin, M. K.; Grätzel, M. *Energy Environ. Sci.* **2009**, *2*, 100–102.
(41) Wang, P.; Klein, C.; Humphry-Baker, R.; Zakeeruddin, S. M.; Grätzel, M. *J. Am. Chem. Soc.* **2005**, *127*, 808–809.
(42) Chen, B.-S.; Chen, K.; Hong, Y.-H.; Liu, W.-H.; Li, T.-H.; Lai, C.-H.; Chou, P.-T.; Chi, Y.; Lee, G.-H. *Chem. Commun.* **2009**, 5844–5846.
(43) Zeng, W.; Cao, Y.; Bai, Y.; Wang, Y.; Shi, Y.; Zhang, M.; Wang, F.; Pan, C.; Wang, P. *Chem. Mater.* **2010**, *22*, 1915–1925.
(44) Mishra, A.; Fischer, M. K. R.; Bäuerle, P. *Angew. Chem., Int. Ed.* **2009**, *48*, 2474–2499.
(45) Marinado, T.; Nonomura, K.; Nissfolk, J.; Karlsson, M. K.; Hagberg, D. P.; Sun, L. C.; Mori, S.; Hagfeldt, A. *Langmuir* **2010**, *26*, 2592–2598.
(46) Hagberg, D. P.; Marinado, T.; Karlsson, K. M.; Nonomura, K.; Qin, P.; Boschloo, G.; Brinck, T.; Hagfeldt, A.; Sun, L. *J. Org. Chem.* **2007**, *72*, 9550–9556.
(47) Bonhôte, P.; Moser, J.-E.; Humphry-Baker, R.; Vlachopoulos, N.; Zakeeruddin, S. M.; Walder, L.; Grätzel, M. *J. Am. Chem. Soc.* **1999**, *121*, 1324–1336.
(48) Robson, K. C. D.; Koivisto, B. D.; Gordon, T. J.; Baumgartner, T.; Berlinguette, C. P. *Inorg. Chem.* **2010**, *49*, 5335–5337.
(49) Abrahamsson, M.; Wolpher, H.; Johansson, O.; Larsson, J.; Kritikos, M.; Eriksson, L.; Norrby, P.-O.; Bergquist, J.; Sun, L.; Akermark, B.; Hammarström, L. *Inorg. Chem.* **2005**, *44*, 3215–3225.
(50) Handa, S.; Wietasch, H.; Thelakkat, M.; Durrant, J. R.; Haque, S. A. *Chem. Commun.* **2007**, 1725–1727.
(51) Haque, S. A.; Handa, S.; Peter, K.; Palomares, E.; Thelakkat, M.; Durrant, J. R. *Angew. Chem., Int. Ed.* **2005**, *44*, 5740–5744.
(52) Karthikeyan, C. S.; Wietasch, H.; Thelakkat, M. *Adv. Mater.* **2007**, *19*, 1091–1095.
(53) Argazzi, R.; Bignozzi, C. A.; Heimer, T. A.; Castellano, F. N.; Meyer, G. J. *J. Am. Chem. Soc.* **1995**, *117*, 11815–11816.
(54) Argazzi, R.; Bignozzi, C. A.; Heimer, T. A.; Castellano, F. N.; Meyer, G. J. *J. Phys. Chem. C* **1997**, *101*, 2591–2597.
(55) Nazeeruddin, M. K.; Péchy, P.; Renouard, T.; Zakeeruddin, S. M.; Humphry-Baker, R.; Comté, P.; Liska, P.; Cevey, L.; Costa, E.; Shklover, V.; Spiccia, L.; Deacon, G. B.; Bignozzi, C. A.; Grätzel, M. *J. Am. Chem. Soc.* **2001**, *123*, 1613–1624.
(56) Medina, A.; Claessens, C. G.; Rahman, G. M. A.; Lamsabhi, A. M.; Mo, O.; Yanez, M.; Guldi, D. M.; Torres, T. *Chem. Commun.* **2008**, 1759–1761.
(57) Anemian, R.; Cupertino, D. C.; Mackie, P. R.; Yeates, S. G. *Tetrahedron Lett.* **2005**, *46*, 6717–6721.
(58) Amthor, S.; Lambert, C. *J. Phys. Chem. A* **2006**, *110*, 1177–1189.
(59) Ash, A. B.; Blumbergs, P.; Markovac, A.; La Montagne, M. P. U.S. Patent 3,7631,488, 1973.
(60) Zhao, L.-X.; Kim, T. S.; Ahn, S.-H.; Kim, T.-H.; Kim, E.-k.; Cho, W.-J.; Choi, H.; Lee, C.-S.; Kim, J.-A.; Jeong, T. C.; Chang, C.-j.; Lee, E.-S. *Bioorg. Med. Chem. Lett.* **2001**, *11*, 2659–2662.
(61) Sasaki, I.; Vendier, L.; Sournia-Saquet, A.; Lacroix, P. G. *Eur. J. Inorg. Chem.* **2006**, 3294–3302.
(62) Frisch, M. J.; Trucks, G. W.; Schlegel, H. B.; Scuseria, G. E.; Robb, M. A.; Cheeseman, J. R.; Montgomery, J. A., Jr.; Vreven, T.; Kudin, K. N.; Burant, J. C.; Millam, J. M.; Iyengar, S. S.; Tomasi, J.; Barone, V.; Mennucci, B.; Cossi, M.; Scalmani, G.; Rega, N.; Petersson, G. A.; Nakatsuji, H.; Hada, M.; Ehara, M.; Toyota, K.; Fukuda, R.; Hasegawa, J.; Ishida, M.; Nakajima, T.; Honda, Y.; Kitao, O.; Nakai, H.; Klene, M.; Li, X.; Knox, J. E.; Hratchian, H. P.; Cross, J. B.; Bakken, V.; Adamo, C.; Jaramillo, J.; Gomperts, R.; Stratmann, R. E.; Yazyev, O.; Austin, A. J.; Cammi, R.; Pomelli, C.; Ochterski, J. W.; Ayala, P. Y.; Morokuma, K.; Voth, G. A.; Salvador, P.; Dannenberg, J. J.; Zakrzewski, V. G.; Dapprich, S.; Daniels, A. D.; Strain, M. C.; Farkas, O.; Malick, D. K.; Rabuck, A. D.; Raghavachari, K.; Foresman, J. B.; Ortiz, J. V.; Cui, Q.; Baboul, A. G.; Clifford, S.; Cioslowski, J.; Stefanov, B. B.; Liu, G.; Liashenko, A.; Piskorz, P.; Komaromi, I.; Martin, R. L.; Fox, D. J.; Keith, T.; Al-Laham, M. A.; Peng, C. Y.; Nanayakkara, A.; Challacombe, M.; Gill, P. M. W.; Johnson, B.; Chen, W.; Wong, M. W.; Gonzalez, C.; Pople, J. A. *Gaussian 03*; Gaussian, Inc.: Wallingford, CT, 2004.
(63) Becke, A. D. *Phys. Rev. A: Gen. Phys.* **1988**, *38*, 3098–3100.
(64) Lee, C.; Yang, W.; Parr, R. G. *Phys. Rev. B: Condens. Matter* **1988**, *37*, 785–789.
(65) Dolg, M.; Stoll, H.; Preuss, H. *Theor. Chem. Acc.* **1993**, *85*, 441–450.
(66) Wedig, M. D.; Stoll, H. *Quantum Chemistry: The Challenge of Transition Metals and Coordination Chemistry*; Kluwer Academic Publishers: Dordrecht, Holland, 1986.
(67) Rassolov, V. A.; Ratner, M. A.; Pople, J. A.; Redfern, P. C.; Curtiss, L. A. *J. Comput. Chem.* **2001**, *22*, 976–984.
(68) Barone, V.; Cossi, M.; Tomasi, J. *J. Chem. Phys.* **1997**, *107*, 3210–3221.
(69) Cossi, M.; Scalmani, G.; Rega, N.; Barone, V. *J. Chem. Phys.* **2002**, *117*, 43–54.
(70) Flamigni, L.; Barbieri, A.; Sabatini, C.; Ventura, B.; Barigelletti, F. *Top. Curr. Chem.* **2007**, *281*, 143–203.
(71) Koops, S. E.; O'Regan, B. C.; Barnes, P. R. F.; Durrant, J. R. *J. Am. Chem. Soc.* **2009**, *131*, 4808–4818.
(72) Karthikeyan, C. S.; Peter, K.; Wietasch, H.; Thelakkat, M. *Sol. Energy Mater. Sol. Cells* **2007**, *91*, 432–439.